Spatial and seasonal variations of leaf area index (LAI) in subtropical secondary forests related to floristic composition and stand characters

Wenjuan Zhu[1,2], Wenhua Xiang[1,2,3*], Qiong Pan[4,1], Yelin Zeng[1], Shuai Ouyang[1,2,3], Pifeng Lei[1,2,3], Xiangwen Deng[1,2,3], Xi Fang [1,2,3], Changhui Peng[5,1]

1 Faculty of Life Science and Technology, Central South University of Forestry and Technology, Changsha 410004, Hunan Province, China

2 Huitong National Field Station for Scientific Observation and Research of Chinese Fir Plantation Ecosystem in Hunan Province, Huitong 438107, China

3 National Engineering Laboratory of Applied Technology for Forestry & Ecology in Southern China, Changsha 410004, China

4 Changsha Environmental Protection College, Changsha 410004, China

5 Institute of Environment Sciences, Department of Biological Sciences, University of Quebec at Montreal, Montreal, QCH3C 3P8, Canada

* *Correspondence to*: Wenhua Xiang, Email: xiangwh2005@163.com, Tel.: +86 0731 85623483

Abstract. Leaf area index (LAI) is an important parameter related to carbon, water and energy exchange between canopy and atmosphere, and is widely applied in process models that simulate production and hydrological cycles in forest ecosystems. However, fine-scale spatial heterogeneity of LAI and its controlling factors have yet to be fully understood in Chinese subtropical forests. We used hemispherical photography to measure LAI values in three subtropical forests (*Pinus massoniana-Lithocarpus glaber* coniferous and evergreen broadleaved mixed forests, *Choerospondias axillaris* deciduous broadleaved forests, and *L. glaber-Cyclobalanopsis glauca* evergreen broadleaved forests) from April 2014 to January 2015. Spatial heterogeneity of LAI and its controlling factors were analysed using geostatistical methods and the generalised additive models (GAMs), respectively. Our results showed that LAI values differed greatly in the three forests and their seasonal variations were consistent with plant phenology. LAI values exhibited strong spatial autocorrelation for the three forests measured in January and for the *L. glaber-C. glauca* forest in April, July and October. Obvious patch distribution pattern of LAI values occurred in three forests during the non-growing period and this pattern gradually dwindled in the growing season. Stem number, crown coverage, proportion of evergreen conifer species on basal area basis, proportion of deciduous species on basal area basis and forest types affected the spatial variations in LAI values in January, while stem number and proportion of deciduous species on basal area basis affected the spatial variations in LAI values in July. Floristic composition, spatial heterogeneity and seasonal variations should be considered for sampling strategy in indirect LAI measurement and application of LAI to simulate functional processes in subtropical

forests.

Keywords: Leaf area index; Spatial heterogeneity; Geostatistical analysis; Generalised additive models (GAMs)

1 Introduction

Many fundamental ecological processes in forest ecosystems, such as carbon (C) flux as well as water and energy exchanges, take place between the canopy layer and atmosphere (GCOS, 2006; Brut et al., 2009; Alonzo et al., 2015; Liu et al., 2015b). At a finer scale, leaves within the canopy are the primary organ to perform a series of physiological activities (i.e. photosynthesis, respiration and evapotranspiration) (Aragão et al., 2005) and physical reactions (i.e. rainfall and radiation interception) (Aston, 1979; Smith, 1981; Crockford & Richardson, 2000). Therefore, the amount of leaves in a forest is the determinant of above-ground ecological processes and ecosystem functions. Leaf area index (LAI), defined as total one-sided leaf area per unit ground surface area (Biudes et al., 2014), is a widely used parameter (Kross et al., 2015) to quantitatively describe the vegetation canopy structure (Woodgate et al., 2015), to simulate ecological process models (Brooks et al., 2006; Sprintsin et al., 2007; Facchi et al., 2010; Gonsamo & Chen, 2014) and to reveal tree growth and productivity in forests at stand scale and landscape level (Lee et al., 2004; Liu et al., 2015b). In addition, LAI is listed as one of the essential variables for observation of global climate (Mason et al., 2003; Manninen et al., 2009) and for remote sensing data validation (Asner et al., 2003; Clark et al., 2008). Thus, accurate estimates of LAI value are

important to understand ecological processes in forest ecosystems.

At present, various direct and indirect methods have been developed to measure LAI in forests. Direct estimation methods including leaf harvest (Clark et al., 2008), allometric equations and litter collection (Ryu et al., 2010; Liu et al., 2015a) are recognised as the most accurate. However, leaf harvest and allometric equations methods need time-consuming, labour-intensive and destructive sampling processes, while litter collection is more feasible for temperate deciduous forests. Obviously, the direct methods are less applicable to large-scale and long-term LAI monitoring (Bequet et al., 2012; Biudes et al., 2014). Indirect methods include using a plant canopy analyser (Licor LAI-2000), hemispherical or fisheye photography (Macfarlane et al., 2007) and remote sensing (Biudes et al., 2014). The indirect methods retrieve LAI value from light transmittance through canopies or from canopy image analysis. For large-scale LAI estimates, remote sensing is the most effective method but requires validation with ground-based LAI data. LAI estimates on the ground at small scales are still a challenge due to the problems of sampling strategies associated with accepted level of accuracy, time and cost considerations (Richardson et al., 2009). Hemispherical photography is a relatively simple and easily operated method among many indirect methods to retrieve LAI value at small scales (Demarez et al., 2008). Correction of the effects of woody materials, clumping and zenith angels or exposure is critical to improve the accuracy of LAI estimation (Liu et al., 2015b). Analysis software development and portable and timely characteristics allow hemispherical photography to measure spatial heterogeneity and seasonal variations of LAI in forests.

77 Forest canopy structure is highly complex so LAI values show great temporal and spatial variations at
78 scales ranging from stand to global scale. For example, LAI values in the 7.9 ha plot of an old humid
79 temperate forest tended to increase spatially as elevation increased and showed a temporal variation
80 with plant phenology (Naithani et al., 2013). The spatial patterns of LAI values at stand scale were
81 significantly influenced by spatial distribution of tree species, which was dependent on topography and
82 soil types (Naithani et al., 2013). The coefficient of variation (CV) in LAI decreased as the scale
83 increased and LAI values did not have any relationship with biome type and climate patterns, but were
84 influenced by land use and land cover, terrain features, and soil properties at stand scale (Aragão et al.,
85 2005). The CV of LAI of three species (i.e. beech, oak and pine) had different degrees of spatial
86 variation in a 1 ha plot at stand level (Bequet et al., 2012). LAI values in sagebrush displayed strong
87 spatial patterns with time after disturbance and increased with stand age and total plant cover (Ewers &
88 Pendall, 2007). The LAI values derived from MODIS data (Myneni et al., 2002; Huang et al., 2008)
89 revealed strong spatial variations at global scale, which were correlated with latitude (Tian et al., 2004).
90 At the global scale, temperature is the limiting factor for LAI under cool conditions while water plays a
91 predominant role under other conditions, and this pattern differed among plant functional types (Iio et
92 al., 2014). The factors that govern the spatial variations in LAI values at stand level include forest types,
93 stand structure (Bequet et al., 2012), climate (Shao & Zeng, 2011), topography, soil moisture condition
94 (Breshears & Barnes, 1999), and human disturbance and management activities (Huang & Ji, 2010).
95 Although effects of topography, soil properties (Aragão et al., 2005; Naithani et al., 2013) and stand

96 characters (Bequet et al., 2012; Yao et al., 2015) on LAI values have been investigated in detail, the
97 effect of forest type, stand structural diversity and stand structure on spatial heterogeneity and seasonal
98 variations of LAI has yet to be fully understood.

99 Chinese subtropical forests contain a diversity of tree species with complex canopy structure that
100 mostly grow on heterogeneous topography and soil conditions. As a result, LAI in subtropical forests
101 may exhibit great spatial and seasonal variations, which is worthy of further investigation. However,
102 LAI data of subtropical forests are relatively deficient in the global database (see Asner et al., 2003). In
103 this study, we selected three different forests: *Pinus massoniana-Lithocarpus glaber* coniferous and
104 evergreen broadleaved mixed forests, *Choerospondias axillaris* deciduous broadleaved forests, and *L.*
105 *glaber-Cyclobalanopsis glauca* evergreen broadleaved forests, in which to measure LAI values were
106 measured by using hemispherical photography. Spatial heterogeneity of LAI was investigated through
107 geostatistical analysis, and generalised additive models (GAMs) were used to examine how stand
108 structural diversity and stand characters affect LAI variations in the three forests. Specifically, the
109 objectives of this study were: (1) to examine differences and seasonal variations in LAI among three
110 forests in subtropical China; (2) to analyse spatial heterogeneity of LAI values within a specific forest;
111 and (3) to identify how forest types, stand structural diversity and stand characters control the spatial
112 heterogeneity and seasonal variations of LAI values in three forests.
113

114 ## 2 Materials and methods

2.1 Study site description

The study was carried out at Dashanchong Forest Farm (latitude 28°23′58″-28°24′ 58″ N, longitude 113°17′46″-113°19′08″ E), Changsha County, Hunan Province, China. The farm experiences a humid mid-subtropical monsoon climate. Mean annual air temperature was 16.5 °C, with a mean monthly minimum temperature of -11°C in January and maximum temperature of 40°C in July. Mean annual precipitation ranged from 1412 mm to 1559 mm, mostly occurring between April and August. The topography is characterized by a typical low hilly landscape with an altitude between 55 m and 260 m above sea level. Soil type is designated as well-drained clay loam red soil developed on slate and shale rock, classified as Alliti-Udic Ferrosols, corresponding to Acrisol in the World Reference Base for Soil Resource (IUSS Working Group WRB, 2006). Evergreen broadleaved forest is the climax vegetation of the region. As a result of human disturbance and management activities, the farm has no primary forest, and possesses a range of secondary forests in different stages of succession (based on species composition) dominated by different tree species, including (1) early stage *P. massoniana-L. glaber* coniferous and evergreen broadleaved mixed forests dominated by the shade-intolerant coniferous species typical of early succession, (2) middle stage *C. axillaris* deciduous broadleaved forests dominated by shade-intolerant deciduous broadleaf species, and (3) late stage *L. glaber-C. glauca* evergreen broadleaved forests dominated by the shade-tolerant evergreen broadleaved species commonly observed in the late stage of succession in this farm (Xiang et al., 2015; Ouyang et al., 2016).

2.2 Determination of stand characteristics

We established a permanent plot for each of three forests (i.e. 90 m × 190 m irregular plot for *P. massoniana-L. glaber* mixed forests, 100 m × 100 m plot for *C. axillaris* deciduous forests, and 100 m × 100 m plot for *L. glaber-C. glauca* evergreen broadleaved forests). Each plot was divided into 10 m × 10 m subplots, where tree species, diameter at breast height (DBH, cm), tree height (H, m), height under the lowest live branch (m) and crown width (m) were measured for the individual stem with DBH larger than 1 cm. Stand characteristics for the trees with DBH >4 cm of the three forests are presented in Table S1.

To identify the factors that control spatial heterogeneity of LAI values in the forests, we selected individual trees with H larger than average height of each stand (see Table S1) and calculated their stem number, average DBH, H, total basal area at breast height (BA), crown width, crown coverage (calculated from crown diameter measured for individual trees within a stand), tree species diversity, tree size diversity, the proportion of BA of three functional group (coniferous, deciduous and evergreen broadleaved species) to total stand BA within a subplot. Tree species diversity (biodiversity index, BDI) was determined using the Shannon-Wiener index as follows:

$$BDI=-\sum P_i \ln P_i \quad (1)$$

where P_i is important value of ith species and is calculated by dividing the sum of relative abundance degree (Ar) and relative dominance degree (Dr) of ith species within a subplot by two.

Based on the Shannon-Wiener index, 2 cm was used for the DBH class, so tree size diversity (H) was

153 determined using the formula of Lei et al. (2009):

154 $$H = -\sum P_i \ln P_i \quad (2)$$

155 where P_i is the proportion of basal area for the ith diameter class.

156

157 **2.3 Sampling design for LAI measurement**

158 At the centre of each subplot of the three forests, hemispherical photographs were taken using a LAI

159 measuring instrument (SY-S01A, Shiya Scientific and Technical Cooperation, Hebei, China) throughout

160 four measurement seasons, i.e. in April (spring), July (summer) and October (autumn) in 2014 and

161 January (winter) in 2015. The operation was carried out below canopy with the fisheye lens (Pentax

162 TS2V114E, Japan) 1.0 m above the ground (Manninen et al., 2009) with a viewing angle of 180°. The

163 picture exposure is automatic exposure set by the manufacturer, and we took the photographs (768 ×

164 494 pix, BMP) in the morning, at dusk or when cloudy, in order to minimize influence of direct

165 sunshine (Rich, 1990; Bequet et al., 2012). The images were processed and effective LAI values (L_e)

166 were recorded using plant canopy analysis software developed by the manufacturer, for which

167 appropriate pixel classification (thresholding) was chosen (752(H) × 494(V)), viewing angle considered

168 (150°), and the hemispherical photography was divided into five rings to obtain results. To obtain

169 accurate LAI (L), the correction was made to L_e based on previous theory (Chen, 1996):

170 $$L = \frac{(1-\alpha) L_e \gamma_E}{\Omega_E} \quad (3)$$

171 where α is the ratio of woody to total area and reflects the contribution of woody materials to L_e, and Ω_E

is the clumping index that quantifies the effect of foliage clumping beyond shoots level. In the method getting accurate Ω_E values, the hemispherical photography was divided into ten sectors. γ_E is the needle to shoot area ratio and quantifies the effect of foliage clumping within shoots.

Photoshop Software (Adobe Photoshop CS5, Adobe Systems Incorporated, North America) was used to calculate α. After total pixel number of L_e image was determined, in the Photoshop software, we used the Clone Stamp Tool to select the image of the woody materials (e.g. stems) and excluded the pixels, leaving only leaves on the photos, recorded as LAI of leaves (LAI_{leaf}). The value of α was calculated accordingly:

$$\alpha = (L_e - LAI_{leaf})/L_e \quad (4)$$

The logarithm averaging method proposed by Lang and Xiang (1986) was applied to calculate Ω_E:

$$\Omega(\theta) = \frac{\ln[P(\bar{\theta})]}{\ln[P(\bar{\theta})]} = \frac{n \ln[P(\bar{\theta})]}{\sum_{k=1}^{n} \ln(P_k(\theta)]} \quad (5)$$

where $P(\theta)$ is the average gap fraction (expressed without the bar in the text), $\ln[P(\theta)]$ is the logarithm average of the gap fraction, and $P_k(\theta)$ is the gap fraction of segment k. For deciduous and evergreen broadleaved species, γ_E=1.0, but for coniferous species, γ_E is always >1.0, but we ignored the effect of needle to shoot area on LAI in this study.

2.4 Data analysis

The minimum, maximum, mean value, standard deviation and CV were calculated for the LAI data measured in 100 plots within each forest. Two-way analysis of variance (ANOVA) was used to detect

191 effect of forest type and measurement season on LAI value. The LAI data in the three forests were
192 tested for normal distribution using the K-S test (P<0.05). We followed Chiang et al. (2003) in
193 regarding LAI values as normal when they fell within the mean value ±3 standard deviations. Otherwise,
194 the LAI values were regarded as outliers and replaced with the maximum or the minimum of normal
195 values. Because the geostatistical analysis requires that the data meet normal distribution, the
196 transformation was applied if the data did not meet normal distribution (Dai et al., 2014). Most values
197 required natural logarithm transformation to meet assumptions of normality. The exception is for *L.*
198 *glaber-C. glauca* in April and in November which were artan-transformed.

199 To investigate spatial heterogeneity of LAI values over four seasons measured in the three forests,
200 semivariance function was calculated as follows:

201 $$\gamma(h) = \frac{1}{2N(h)} \sum_{i=1}^{N(h)} [Z(x_i) - Z(x_i + h)]^2 \qquad (6)$$

202 where $\gamma(h)$ is semivariance value of lag distance h, $N(h)$ is the number of pair data for lag distance h,
203 $Z(x_i)$ and $Z(x_i + h)$ represent LAI values at coordinate x_i and (x_i+h) (Rossi et al., 1992). Based on the
204 semivariogram plotting $\gamma(h)$ values against h variable, the appropriate models were fitted and we
205 obtained the values of nugget (C_0), sill (C_0+C), range (A_0) (Ewers & Pendall, 2007) and the ratio
206 $[C/(C_0+C)]$ that reflected the degree of spatial autocorrelation of LAI values in a forest. Because spatial
207 autocorrelation and semivariogram theory make unbiased optimal estimation for regional variables in a
208 limited area (Bivand et al., 2013), the Kriging interpolation method, an unbiased estimation of the
209 regional variables of the sampling points using the structure of the data and semivariogram function,

was used to predict unknown LAI values in the forests from the data measured and to produce spatial distribution maps of LAI values for the three forests and four seasons. Compared with other methods, the Kriging method can overcome the difficulty in analysing error of interpolation, does not produce the boundary effect of regression analysis, and estimates the spatial variability distribution of measured parameters. Ordinary Kriging - one of the Kriging methods - is a least-squares method of spatial prediction based on the assumption of an unknown mean. It is the most common type of Kriging in practice (Dai et al., 2014) and is widely used in soil spatial heterogeneity studies (Elbasiouny et al., 2014). In our study, we also used the ordinary Kriging interpolation method to investigate spatial heterogeneity of LAI values.

Because the largest amount of defoliated leaves occurs in January and leaves fully expand in July in subtropical forests, we chose LAI values measured in January and July in three forests as response variables. The explanatory variables include forest types, stand structural diversity (species richness, tree species diversity and tree size diversity) and stand characters (stem number, average DBH, H, BA, crown width, crown coverage, the proportion of two functional groups (deciduous and evergreen conifer species) to total stand BA). The generalised additive models (GAMs) are able to analyse complex and nonlinear relationships (Guisan et al., 2002; Austin, 2002; Wood, 2006). Therefore, we used GAMs to examine how the factors affect LAI values. The function of GAMs is the addition of many smooth functions and each smooth function has an explanatory variable. In our study, we chose smooth spline with two splines as the smooth method for GAMs. The variance inflation factor (VIF) - the ratio of the

229 regression coefficient variance for a variable when fit with all variables to that for the variable if fit on
230 its own - was used to test the multi-collinearity of explanatory variables (James et al., 2013). When the
231 VIF of an explanatory variable is between 0 and 10, the variable was retained to the model; otherwise,
232 we discarded the variable (Shen et al., 2015). The Akaike information criterion (AIC) or generalised
233 cross validation (GCV) was used to determine whether the model was good or bad (Clark, 2013). The
234 factors selected after the multi-collinearity test were used for multi-factor analysis. After all the possible
235 models in multi-factor analysis, we determined the optimal model based on the significant influence of
236 all explanatory variables in the model with the smallest AIC or GCV (Dong et al., 2012). Geostatistical
237 analysis was performed with GS+ software (Gamma Design Software). Statistical analysis and GAMs
238 analysis were operated in R 3.2.1 (R Development Core Team, 2015). The car packages were used to
239 test multi-collinearity and the gam packages were used to select the optimal model.
240

241 # 3 Results

242 ## 3.1 Variation in LAI values

243 The LAI values varied with forest type and measurement season (Table 1). Generally, LAI differed
244 significantly between measurement season (P<0.001), but LAI difference was not significant among
245 forest types (P>0.05). Interactive effects of measurement seasons and forest types on LAI were
246 significant (P<0.01). Among three forests, LAI in the *P. massoniana-L. glaber* forest had relatively low
247 variation, while LAI in the *L. glaber-C. glauca* forest had the highest variation. In the *P. massoniana-L.*

glaber forest, LAI showed the largest variation (the highest CVs) in October and the lowest variation (the smallest CVs) in January. In the *C. axillaris* forest, the largest variation in LAI was found in April and the lowest was found in January. In the *L. glaber-C. glauca* forest, LAI showed the largest variation in April and had the lowest variation in July.

Mean LAI values in the three forests showed different seasonal variation patterns (Fig. 1). The *C. axillaris* forest exhibited a unimodal pattern of seasonal variation, with the maximum mean LAI value (3.11±1.18) occurring in July and the minimum mean LAI value (1.28±0.44) in January. In the *P. massoniana-L. glaber* forest and *L. glaber-C. glauca* forest, the maximum mean LAI values occurred in October and the minimum mean LAI values appeared in January. During the growing season (April and July), the *C. axillaris* forest had the highest mean LAI value and the *L. glaber-C. glauca* forest had the lowest mean LAI value. During the non-growing season (October and January), the *L. glaber-C. glauca* forest had the highest mean LAI value in January, while the *P. massoniana-L. glaber* forest had the highest mean LAI value in October, and the *C. axillaris* forest had the lowest mean LAI values.

Mean α values in the three forests showed different seasonal variation patterns (Table 2). The *C. axillaris* forest exhibited a unimodal pattern of seasonal variations in mean α value, with the maximum mean α value occurring in January and the minimum mean α value in July. No obvious seasonal variations were found for the mean α value in the *P. massoniana-L. glaber* forest and in the *L. glaber-C. glauca* forest. Mean Ω_E values in the three forests were between 0.84 and 0.92, but they did not show clear seasonal variations, and the standard deviations were small.

3.2 Spatial heterogeneity in LAI values

The semivariogram results for LAI across the three forests during different measurement seasons are summarised in Table 3. The spatially dependent variance [C] accounted for 88.9%-98.4% of the total variance [$C+C_0$] for LAI values measured in January in the three forests and also in April, July and October in the *L. glaber-C. glauca* forest. This indicated the strong spatial autocorrelations of LAI values over short distances. These LAI data were best fitted with a Gaussian model or exponential model ($r^2>0.50$).

Spatial autocorrelation ranges of LAI values differed among forests and measurement seasons (Table 3). In January, the largest spatial autocorrelation range was found in the *P. massoniana-L. glaber* forest, and the lowest was found in the *C. axillaris* forest. In April, the largest spatial autocorrelation range of LAI was found in the *C. axillaris* forest, and the lowest was found in the *P. massoniana-L. glaber* forest. In July, the largest spatial autocorrelation range of LAI was in the *P. massoniana-L. glaber* forest, while the smallest was in the *C. axillaris* forest. In October, the largest spatial autocorrelation range of LAI was in the *L. glaber-C. glauca* forest, while the smallest was in the *P. massoniana-L. glaber* forest. Seasonal changes of range showed one peak pattern for *C. axillaris* forest and *L. glaber-C. glauca* forest, where the large range appeared in the growing season (April and July) and the small range appeared in the non-growing season (October and January).

Spatial distribution pattern of LAI values also varied with forest type and measurement season (Fig.

2). For example, LAI values in January across the three forests exhibited obvious patch and heterogeneous spatial distribution. In April and July, less spatial heterogeneity was found for LAI values especially in the *P. massoniana-L. glaber* forest. In October, heterogeneous and patch spatial distributions of LAI values appeared in the *L. glaber-C. glauca* forest, and banded spatial distributions of LAI values obviously appeared in the *C. axillaris* forest.

3.3 Factors affecting LAI variation

The multi-collinearity test indicated that the explanatory variables in January and July did not have multi-collinearity. Thus, forest type, species richness, tree species diversity, tree size diversity, stem number, average DBH, H, BA, crown width, crown coverage, and the proportion of two functional groups (deciduous and evergreen conifer species) to total stand BA were included as explanatory variables in multi-factor analysis for LAI values measured in January in the three forests. After comparing all possible models, the best fitted GAMs for LAI values in January were expressed as LAI ~ s(stem number, 2) + s(crown coverage, 2) + s(PESB, 2) + s (PDSB, 2) + factor (forest types) (Table 4). For LAI values measured in July, all these factors selected by the multi-collinearity test were included as explanatory variables in multi-factor analysis. The best fitted GAMs for LAI values in July were expressed as LAI ~ s(stem number, 2) + s(PDSB, 2) (Table 4).

The explanatory variables included in GAMs reflected their effects on or relationship with LAI variations. Given that other variables were fixed, LAI measured in January tended to decrease as stem

number increased. LAI showed a positive nonlinear relationship with crown coverage up to ~200 m^2, and then decreased with increasing crown coverage. The LAI values tended to increase as the proportion of evergreen conifer species to total stand BA increased, and tended to decrease as the proportion of deciduous species to total stand BA increased (Fig. 3). Given that other variables were fixed, LAI measured in July tended to increase as stem number increased up to ~7 and then decreased at higher values. The effect of the proportion of deciduous species to total stand BA on LAI appeared more complicated, in that LAI increased as the proportion of deciduous species to total stand BA increased up to ~0.7, and then decreased at higher values (Fig. 4).

4 Discussion

4.1 Seasonal variation in LAI value among forest type

LAI data in subtropical forests in southern China are lacking compared to other global regions (Asner et al., 2003). This study provided seasonal LAI data in three subtropical forests that consist of contrasting functional types of species. Their mean LAI values varied from 1.28±0.44 to 3.28±1.26 (Table 1). This result is close to the LAI range (from 1.0 in winter to 4.0 in summer) retrieved by remote sensing techniques from the subtropical area of China from 2000 to 2010 (Liu et al., 2012). Compared with the LAI values estimated from allometric equations (Xiang et al., 2016) and specific leaf area (SLA) values in 40 m × 40 m plots in this study (5.29-9.19), the LAI values measured by hemispherical photography are low but significantly correlated (r^2=0.40 and P=0.035). Previous studies (see Lopes et

al., 2015) have proved the underestimation of LAI using hemispherical photography. However, the method is feasible to obtain forest LAI data and to investigate spatial and seasonal variation in such values (Coops et al., 2004; Dovey & Toit, 2006).

The ratio of woody to total area (α) and the clumping index (Ω_E) have been recognised as the error sources in LAI measurement by optical methods (Chen et al., 1997; Bréda, 2003; Liu et al., 2015a). So far these two parameters have been measured in northeastern China (Liu et al., 2015a; Liu et al., 2015b), which showed that the α values ranged from 0.04±0.01 to 0.69±0.12 and Ω_E values ranged from 0.88±0.04 to 0.96±0.01. These values were measured in temperate forest in northeastern China and differed from our study (mean α values varied from 0.04±0.03 to 0.15±0.09 and mean Ω_E values varied from 0.84±0.09 to 0.92±0.08) (Table 2), so they are not suitable for LAI correction in subtropical forests. Also literature on α and Ω_E values in subtropical forests is scarce. The variations in α are probably due to the seasonal variations and spatial heterogeneity of canopy structure in the three forests. In general, the α values are consistent with the amount of leaf litter. Our results showed that the large mean α values occurred in autumn for the *P. massoniana-L. glaber* forest and the *C. axillaris* forest, but in spring and autumn for the *L. glaber-C. glauca* forest (Table 2). This seasonal change in mean α value in three forests was generally consistent with the amount of leaf litter collected by a litter trap installed in each forest type (Guo et al., 2015). The average Ω_E value (0.87) in this study was smaller than the values of mixed broadleaved-Korean pine forest in northeastern China (Liu et al. 2015b) and this could be attributed to the different region and forests. The values of α and Ω_E obtained in this study fill the gap

of calibration for optical measurement of LAI in subtropical forests.

Mean LAI values differed among the three forests and the differences were significant between the *C. axillaris* forest and the other two forests at a given measurement season. The *C. axillaris* forest had a relatively high mean LAI value during the growing season but changed to the lowest mean LAI value during the non-growing season. The change in mean LAI values in the *C. axillaris* forest was consistent with the study of a deciduous species-dominated forest reported by Naithani et al. (2013). It has been reported that the forests consisting of different plant functional types showed different LAI values (Asner et al., 2003; Iio et al., 2014). The differences and seasonal variations of LAI values in the three forests could be attributed to floristic composition and phenological defoliation patterns of tree species especially the deciduous species. The *C. axillaris* forest consisted of 74.15% deciduous species, 25.80% evergreen broadleaved species and 0.05% evergreen coniferous species, while the proportions of deciduous species were 10.05% and 25.70% in the *P. massoniana-L. glaber* and *L. glaber-C. glauca* forests, respectively. Seasonal growth and defoliation of different functional types of species lead to the change in leaf lifespan and foliage area (Niinemets, 2010) during different seasons related to temperature and water availability, which are responsible for the unimodal pattern of seasonal variation in mean LAI values. This agrees with the results of Liu et al. (2012), where the highest LAI was found in summer (July), followed by autumn (October) and spring (April), and the lowest was found in winter (January).

362 **4.2 Within-forest spatial heterogeneity and factors controlling LAI**

363 Semivariograms of LAI values in the three forests were fitted with spherical, Gaussian, exponential
364 or linear models (Table 3). Based on the fitted models, the degree of spatial autocorrelation could be
365 evaluated. Spatial autocorrelation is weak when the determination coefficient (r^2) of the best-fitted
366 semivariogram model is less than 0.5 (Duffera et al., 2007). The ratio [$C/(C_0+C)$] is also used to
367 describe the degree of spatial autocorrelation. A ratio of between 0 and 0.25 indicates a weak spatial
368 autocorrelation, of between 0.26 and 0.75 indicates moderate autocorrelation and of more than 0.75
369 indicates strong autocorrelation (Lopez-Granados et al., 2004). Spatial autocorrelation of LAI in this
370 study varied with forest and measurement season (Table 3). Strong spatial autocorrelation in LAI values
371 at a short range measured in January in all three forests indicated the sampling distance is reasonable for
372 LAI variables within the spatial range (Liu et al., 2008). On the contrary, weak autocorrelation indicated
373 that more samples and smaller sampling intervals should be taken to determine spatial dependency of
374 LAI, such as for LAI measured in April in the *P. massoniana-L. glaber* forest.

375 Spatial heterogeneity in LAI values was different for forest type and measurement season. Our study
376 described spatial variations in LAI value by CV and geostatistical analysis, and the results were largely
377 consistent with each other. In general, the CVs of LAI values in the three forest types (in particular *C.*
378 *axillaris* forest) were higher for the period of leaf onset (April) and senescence (October) than for the
379 period of leaf maturity (July) (Table 1). This reflects changes in leaves due to plant phenology and is
380 consistent with the study of Naithani (2013) where LAI became increasingly homogenous from leaf

onset to maturity, but became more heterogeneous from maturity to senescence. As a result, degree of heterogeneity in LAI value for all three forests tended to dwindle from leaf non-growing season to growing season (Fig. 2).

The complex hydrothermal environment results in complex vertical and horizontal variation in canopy layer and formed unique spatial heterogeneity in LAI values. The effects of stand characters on LAI have been examined and positive and negative effects have been reported (Tobin et al., 2006; Bequet et al., 2012; Yao et al., 2015). In our study, results from GAMs showed that forest types, stand structural diversity and stand characters affected spatial heterogeneity of LAI values significantly in the three forests. This finding that floristic composition and stand characters affected LAI values measured in July is consistent with the study of Yao et al. (2015); LAI values increased with stem number but when stem number was larger than 7, LAI values decreased with stem number mainly due to the floristic composition in these study areas. Because July is the period of leaf maturity for deciduous species and leaves fully expand in this season, LAI values tended to increase as ratio of deciduous species increased, but when the ratio was higher than ~0.7, its negative relationship with LAI probably could be explained by the strong competition among tree species, with diverse species composition and the canopy overlap among tree species (Fig. 4). Our results indicated that LAI values did not exhibit a significant relationship with stand BA, consistent with the findings of Mcdowell (2007); total LAI did not exhibit a clear pattern in relation to stand BA.

Until now, the non-growing season relationship of LAI variation with forest type and stand characters

has been seldom reported. In this study, forest type, stem number, crown coverage, proportion of evergreen conifer species to total stand BA and proportion of deciduous species to total stand BA and forest type were the factors significantly affecting LAI variation in January. As January is mainly the leaf senescence period of deciduous species, LAI values in January decreased with stem number and decreased with deciduous species ratio. The relationship between LAI value and the evergreen species ratio was generally the reverse of that between LAI and the deciduous species ratio. The fact that LAI values in January decreased with increasing crown coverage when crown coverage was larger than ~200 m^2 could be explained by large crown coverage resulting in more defoliation (in particular for deciduous species) in the forest in January (Fig. 3). The proportion of deciduous species to total stand BA both significantly affected LAI variations in January and July, and the relationship between LAI and the deciduous species proportion was reversed when the ratio was smaller than 0.7 in these two seasons, which is consistent with the growth law of deciduous species. Thus, deciduous species play an important role in LAI variations across seasons. Also the seasons have a significant effect on LAI variation by affecting leaf growth. The partial effects of stem number and crown coverage on the LAI values observed in January showed these smooth functions were large at both ends of the 95% confidence interval. This was due to the small sample number in this range, and most were concentrated in the middle parts, the same as the partial effects of stem number on the LAI values observed in January (Figs 3, 4).

Although the factors selected by regression could explain a small proportion (4%) of spatial

heterogeneity of LAI measured in July, the factors selected in January could explain 35% of the LAI spatial heterogeneity (Table 4). The LAI heterogeneity also could be affected by several other factors, such as the topography (Naithani et al., 2012), soil feature (Chloer et al., 2010), soil temperature (Vitasse et al., 2009; Hardwick et al., 2015), microclimate, human activity and other physicochemical properties. However, full leaf expansion of all tree species, which covers up the effect of other physicochemical properties on LAI, leads to a small difference in LAI in July. The effects of environmental factors (e.g. temperate and rainfall) on LAI in the forests at the fine scale should be taken into account in future studies.

Spatial heterogeneity of LAI in the three forests can yield some useful information for sampling strategy to accurately estimate of LAI using indirect measurement. An optimal sampling strategy should consider appropriate sampling plot size and the lowest sampling number that, as far as possible, obtains a high sampling accuracy and a low sampling error (Bequet et al., 2012). Our study found that strong spatial autocorrelations range were ~13-27 m (the minimal range was 13.80 m, and the maximal range was 27.00 m) (Table 3), indicating that the range from 13 m to 27 m might serve as the reference for sampling plot size to estimate LAI in subtropical forests. In addition, LAI heterogeneity was closely related to floristic composition and stand characters, thus stand structural variables (BA or DBH) are important for sampling strategy to measure LAI in forests (Bequet et al., 2012).

5 Conclusions

This study measured LAI in three subtropical forests using a hemispherical photography method over four seasons, and offered reliable data to analyse spatial and seasonal variations in LAI. Our results indicated that LAI differed greatly with forest type and measurement season. Seasonal variation in LAI across the three forests reflects defoliation due to plant phenology. LAI values for all three forests exhibited different spatial autocorrelation in the four seasons. A clear patch distribution pattern in LAI value was found during the non-growing seasons and this pattern gradually dwindled in the growing seasons. While stem number, crown coverage, proportion of evergreen conifer species to total stand BA, the proportion of deciduous species to total stand BA, and forest type significantly affected spatial variations in LAI values in January, stem number and proportion of deciduous species to total stand BA significantly affected spatial variations in LAI values in July. These findings supplement LAI data for global synthesis, and will provide valuable information for sampling strategies to enable more accurate estimates of LAI for simulated models of production and hydrological cycles in subtropical forests.

Acknowledgements

This study was supported by the Specialized Research Fund for the Doctoral Program of Higher Education (20124321110006), the National Natural Science Foundation of China (31570447 and 31300524), the Programme of State Forestry Special Fund for Public Welfare Sectors of China (201304317), and the New Century Excellent Talents Program (NCET-06-0715). Thanks also go to the staff of the administration office of Dashanchong Forest Farm, Changsha County, Hunan Province,

for their local support.

References

Alonzo, M., Bookhagen, B., McFadden, J. P., Sun, A., and Roberts, D. A.: Mapping urban forest leaf area index with airborne lidar using penetration metrics and allometry, Remote Sens. Environ., 162, 141-153, 2015.

Aragão, L. E., Shimabukuro, Y. E., Santo, F., and Williams, M.: Landscape pattern and spatial variability of leaf area index in Eastern Amazonia, For. Ecol. Manage., 211, 240-256, 2005.

Asner, G. P., Scurlock, J. M. O., and Hicke, J. A.: Global synthesis of leaf area index observations: implications for ecological and remote sensing studies, Global Ecol. Biogeogr., 12, 191-205, 2003.

Aston, A. R.: Rainfall interception by eight small trees, J. Hydrol., 42, 383-396, 1979.

Austin, M. P.: Spatial prediction of species distribution: an interface between ecological theory and statistical modelling, Ecol. Model., 157, 101-118, 2002.

Bequet, R., Campioli, M., Kint, V., Muys, B., Bogaert, J., and Ceulemans, R.: Spatial variability of leaf area index in homogeneous forests relates to local variation in tree characteristics, For. Sci., 58, 633-640, 2012.

Biudes, M. S., Machado, N. G., Danelichen, V. H. M., Souza, M. C., Vourlitis, G. L., and Nogueira, J. S.: Ground and remote sensing-based measurements of leaf area index in a transitional forest and seasonal flooded forest in Brazil, Int. J. Biometeorol., 58, 1181-1193, 2014.

476 Bivand, R. S., Pebesma, E. J., and Gómez-Rubio, V.: Applied spatial data analysis with R, Springer,
477 New York, USA, 2013.
478 Bréda, N. J. J.: Ground-based measurements of leaf area index: a review of methods, instruments and
479 current controversies, J. Exp. Bot., 54, 2403-2417, 2003.
480 Breshears, D. D., and Barnes, F. J.: Interrelationships between plant functional types and soil moisture
481 heterogeneity for semiarid landscapes within the grassland/forest continuum: a unified conceptual
482 model, Landscape Ecol., 14, 465-478, 1999.
483 Brooks, J. R., Meinzer, F. C., Warren, J. M., Domeo, J. C., and Coulombe, R.: Hydraulic redistribution
484 in a Douglas-fir forest: lessons from system manipulation, Plant Cell Environ., 29, 138-150, 2006.
485 Brut, A., Rüdiger, C., Lafont, S., Roujean, J. L., Calvet, J. C., Jarlan, L., Gibelin, A. L., Albergel, C.,
486 Moigne, P. L., Soussana, J. F., Klumpp, K., Guyon, D., Wigneron, J. P., and Ceschia, E.:
487 Modelling LAI at a regional scale with ISBA-A-gs: comparison with satellite-derived LAI over
488 southwestern France, Biogeosciences, 6, 1389-1404, 2009.
489 Chen, J. M.: Optically-based methods for measuring seasonal variation of leaf area index in boreal
490 conifer stands, Agic. For Meteorol., 80, 135-163, 1996.
491 Chen, J. M., Rich, P. M., Gower, S. T., Norman, J. M., and Plummer, S.: Leaf area index of boreal
492 forests: theory, techniques, and measurements, J. Geophys. Res., 102, 29429-29443, 1997.
493 Chloer, P., Sea, W., Briggs, P., Raupach, M., and Leuning, R.: A simple ecohydrological model captures
494 essentials of seasonal leaf dynamics in semiarid tropical grasslands, Biogeosciences, 7, 907-920,

2010.

Chiang, L. H., Pell, R. J., Seasholtz, M. B.: Exploring process data with the use of robust outlier detection algorithms, J. Process Contr., 13(5), 437-449, 2003.

Clark, D. B., Olivas, P. C., Oberbauer, S. F., Clark, D. A., and Ryan, M. G.: First direct landscape-scale measurement of tropical rain forest leaf area index: a key driver of global primary productivity, Ecology Letter, 11, 163-172, 2008.

Clark, M.: Generalized additive models: getting started with additive models in R, Center of Social Research, University of North Dame, Notre Dame, IN, USA, pp.13, 2013.

Crockford, R. H., and Richardson, D. P.: Partitioning of rainfall into throughfall, stemflow and interception: effect of forest type, ground cover and climate, Hydrol. Proc., 14, 2903-2920, 2000.

Coops, N. C., Smith, M. L., Jacobsen, K. L., Martin, M., and Ollinger, S.: Estimation of plant and leaf area index using three techniques in a mature native eucalypt canopy, Austral Ecol., 29, 332-341, 2004.

Dai, F. Q., Zhou, Q. G., Lv, Z. Q., Wang, X. M., and Liu, G. C.: Spatial prediction of soil organic matter content integrating artificial neural network and ordinary kriging in Tibetan Plateau, Ecol. Indic., 45, 184-194, 2014.

Demarez, V., Duthoit, S., Baret, F., Weiss, M., and Dedieu, G.: Estimation of leaf area and clumping indexes of crops with hemispherical photographs, Agr. For. Meteorol., 148, 644-655, 2008.

Dong, X. H., Bennion, H. E., Maberly, S. C., Sayer, C. D., Simpson, G. L., and Battarbee, R. W.:

514 Nutrients exert a stronger control than climate on recent diatiom communities in Esthwaite Water:
515 Evidence from monitoring and palaeolimnological records, Freshwater Biol., 57, 2044-2056, 2012.
516 Dovey, S. B., and Toit, B. D.: Calibration of LAI-2000 canopy analyser with leaf area index in a young
517 eucalypt stand, Trees, 20, 273-277, 2006.
518 Duffera, M., White, J. G., and Weisz, R.: Spatial variability of Southeastern U. S. Coastal Plain soil
519 physical properties: implication for site-specific management, Geoderma, 137, 327-339, 2007.
520 Ewers, B. E., and Pendall, E.: Spatial patterns in leaf area and plant functional type cover across
521 chronosequences of sagebrush ecosystems, Plant Ecol., 194, 67-83, 2007.
522 Elbasiouny, H., Abowaly, M., Abu_Alkheir, A., Gad, A.: Spatial variation of soil carbon and nitrogen
523 pools by using ordinary Kriging method in an area of north Nile Delta, Egypt, Catena, 113, 70-78,
524 2014.
525 Facchi, A., Baroni, G., Boschetti, M., and Gandolfi, C.: Comparing optical and direct methods for leaf
526 area index determination in a maize crop, J. Agri. Eng., 1, 27-34, 2010.
527 Global Climate Observing System (GCOS): Systematic Observation Requirements for Satellite-Based
528 Products for Climate Supplemental details to the satellite-based component of the Implementation
529 Plan for the Global Observing System for Climate in Support of the UNFCCC (2010 Update).
530 WMO/TD: 138. http://www.wmo.int/ pages/prog/gcos/Publications/gcos-154.pdf (accessed on 13
531 November 2012), 2006.
532 Gonsamo, A., and Chen, J. M.: Continuous observation of leaf area index at Fluxnet - Cananda sites,

533 Agric. For. Meteorol., 189, 168-174, 2014.
534 Guisan, A., Edwards, Jr. T. C., and Hastie, T.: Generalized linear and generalized additive model in
535 studies of species distributions: Setting the scene, Ecol. Model., 157, 89-100, 2002.
536 Guo, J., Yu, L. H., Fang, X., Xiang, W. H., Deng, X. W., and Lu, X.: Litter production and turnover in
537 four types of subtropical forests in China, Acta Ecol. Sinica, 35, 4668-4677, 2015. (in Chinese with
538 English abstract)
539 Hardwick, S. R., Toumi, R., Pfeifer, M., Turner, E. C., Nilus, R., and Ewers, R. M.: The relationship
540 between leaf area index and microclimate in tropical forest and oil palm plantation: Forest
541 disturbance drives changes in microclimate, Agric. For. Meteorol., 201, 187-195, 2015.
542 Huang, D., Knyazikhin, Y., Wang, W., Deering, D. W., Stenberg, P., Shabanov, N., Tan, B., and
543 Myneni, R. B.: Stochastic transport theory for investigating the three-dimensional canopy structure
544 from space measurements, Remote Sens. Environ., 112, 35-50, 2008.
545 Huang, M., and Ji, J. J.: The spatio-temporal distribution of LAI in China-the comparison with
546 mechanism model and remote sensing inversion, Acta Ecol. Sinica, 30, 3057-3064, 2010. (in
547 Chinese with English abstract)
548 Iio, A., Hikosaka, K., Anten, N. P. R., Nakagawa, Y., and Ito, A.: Global dependence of field-observed
549 leaf area index in woody species on climate: a systematic review, Global Ecol. Biogeogr., 23,
550 274-285, 2014.
551 IUSS Working Group WRB: World Reference Base for Soil Resource 2006, In: World Soil Resources

552 Reports No. 103. 2nd ed. FAO, Rome, 2006.
553 James, G., Witten, D., Hastie, T., and Tibshirani, R.: An introduction to statistical learning with
554 applications in R. Springer, New York, 2013.
555 Kross, A., McNairn, H., Lapen, D., Sunohara, M., and Champagne, C.: Assessment of RapidEYE
556 vegetation indices for estimation of leaf area index and biomass in corn and soybean crops, Int. J.
557 Appl. Earth Obs. Geoinformation, 34, 235-248, 2015.
558 Lang, A. R. G., and Xiang, Y.: Estimation of leaf area index from transmission of direct sunlight in
559 discontinuous canopies, Agric. For. Meteorol., 35, 229-243, 1986.
560 Lee, K. S., Cohen, W. B., Kennedy, R. E., Maiersperger, T. K., and Gower, S. T.: Hyperspectral versus
561 multispectral data for estimating leaf area index in four different biomes, Remote Sens. Environ., 91,
562 508-520, 2004.
563 Lei, X. D., Wang, W. F., Peng, C. H.: Relationships between stand growth and structural diversity in
564 spruce-dominated forests in New Brunswick, Canada, Can. J. For. Res., 39, 1835-1847, 2009.
565 Liu, X. L., Zhao, K. L., Xu, J. M., Zhang, M. H., Si, B., and Wang, F.: Spatial variability of soil organic
566 matter and nutrients in paddy fields at various scales in southeast China, Environ. Geol., 53,
567 1139-1147, 2008.
568 Liu, Y. B., Ju, W. M., Chen, J. M., Zhu G. L., Xing, B. L., Zhu, J. F., and He, M. Z.: Spatial and
569 temporal variations of forest LAI in China during 2000-2010, Chin Sci Bull., 57, 2846-2856, 2012..
570 Liu, Z. L., Jin, G. Z., Chen, J. M., and Qi, Y. J.: Evaluating optical measurements of leaf area index

against litter collection in a mixed broadleaved-Korean pine forest in China, Trees, 29, 59-73, 2015a.

Liu, Z. L., Wang, C. K., Chen, J. M., Wang X. C., and Jin, G.Z.: Empirical models for tracing seasonal changes in leaf area index in deciduous broadleaf forests by digital hemispherical photography, For. Eco. Manage., 351, 67-77, 2015b.

Lopes, D., Nunes, L., Walford, N., Aranha, J., Sette Jr, C., Viana, H., and Hernandez, C.: A simplified methodology for the correction of Leaf Area Index (LAI) measurements obtained by ceptometer with reference to *Pinus* Portuguese forests, iForest–Biogeosci. Forest., 7: 186-192, 2015.

Lopez-Granados, F., Jurado-Exposito, M., Alamo, S., and Garcia-Torres, L.: Leaf nutrient spatial variability and site-specific fertilization maps within olive (*Olea europaea* L.) orchards, Eur. J. Agron., 21, 209-222, 2004.

Macfarlane, C., Hoffman, M., Eamus, D., Kerp, N., Higginson, S., McMurtrie, R., and Adams, M.: Estimation of leaf area index in eucalypt forest using digital photography, Agr. For. Meteorol., 143, 176-188, 2007.

Manninen, T., Korhonen, L., Voipio, P., Lahtinen, P., and Stenberg, P.: Leaf area index (LAI) estimation of boreal forest using wide potics airborne winter photos, Remote Sens., 1, 1380-1394, 2009.

Mason, P. J., Manton, M., Harrison, D. E., Belward, A., Thomas, A. R., and Dawson, A.: The second report on the adequacy of the global observing systems for climate in support of the UNFCCC. GCOS-82, WMO/TD No. 1143; United Nations Environment Programme; International Council for

590 Science, World Meteorological Organization: Geneva, Switzerland, 2003, p. 74, 2003.
591 Mcdowell, N. G., Adams, H. D., Bailey, J. D., and Kolb, T. E.: The role of stand density on growth
592 efficiency, leaf area index, and resin flow in southwestern ponderosa pine forests, Can. J. For. Res.,
593 37, 343-355, 2007.
594 Myneni, R. B., Hoffman, S., Knyazikhin, Y., Privette, J. L., Glassy, J., Tian, Y., Wang, Y., Song, X.,
595 Zhang, Y., Smith, G. R., Lotsch, A., Friedl, M., Morisette, J. T., Votava, P., Nemani, R. R., and
596 Running, S. W.: Global products of vegetation leaf area and fraction absorbed PAR from year one
597 of MODIS data, Remote Sens. Environ., 83, 214-231, 2002.
598 Naithani, K. J., Baldwin, D. C., Gaines, K. P., Lin, H., and Eissenstat, D. M.: Spatial distribution of tree
599 species governs the spatio-temporal interaction of leaf area index and soil moisture across a forested
600 landscape, PLoS One, 8(3), e58704, 2013.
601 Naithani, K. J., Ewers, B. E., and Pendall, E.: Sap flux-scaled transpiration and stomatal conductance
602 response to soil and atmospheric drought in a semi-arid sagebrush ecosystem, J. Hydrol., 25,
603 176-185, 2012.
604 Niinemets, Ü.: A review of light interception in plant stands from leaf to canopy in different plant
605 functional types and in species with varying shade tolerance, Ecol. Res., 25, 693-714, 2010.
606 Ouyang, S., Xiang, W. H., Wang, X. P., Zeng, Y. L., Lei, P. F., Deng, X. W., Peng, C. H.: Significant
607 effects of biodiversity on forest biomass during the succession of subtropical forest in south China,
608 For. Ecol. Manage., 372, 291-302, 2016.

609 R Development Core Team: R: A language and environment for statistical computing, R Foundation for
610 Statistical Computing, Vienna, Austria, 2015.
611 Rich, P. M.: Characterizing plant canopies with hemispherical photographs, Remote Sens. Rev., 5,
612 13-29, 1990.
613 Richardson, J., Moskal, L. M., and Kim H.: Modeling approaches to estimate effective leaf area index
614 from aerial discrete-return LIDAR, Agr. For Meteorol., 149, 1152-1160, 2009.
615 Rossi, R. E., Mulla, D. J., Journel, Á. G., and Franz, E. H.: Geostatistical tools for modeling and
616 interpreting ecological spatial dependence, Ecol. Monogr., 62, 277-314, 1992.
617 Ryu, Y., Nilson, T., Kobayashi, H., Sonnentag, O., Law, B. E., and Baldocchi, D. D.: On the correct
618 estimation of effective leaf area index: dose it reveal information on clumping effects, Agric. For
619 Meteorol., 150, 463-472, 2010.
620 Shao, P., and Zeng, X. D.: Spatiotemporal relationship of leaf area index simulated by CLM3.0-DGVM
621 and climatic factors, Acta Ecol. Sinica, 16, 4725-4731, 2011. (in Chinese with English abstract)
622 Shen, C. C., Lei, X. D., Liu, H. Y., Wang, L., and Liang, W. J.: Potential impacts of regional climate
623 change on site productivity of *Larix olgensis* plantations in northeast China, iForest-Biogeosci.
624 Forest., e1-10, 2015.
625 Smith, H.: Light quality as an ecological factor. In: Grace, J., E.D. Ford, and P.G. Jarvis (eds). Plants
626 under their atmospheric environment, Blackwell, Oxford, 93-110, 1981.
627 Sprintsin, M., Karnieli, A., Berliner, P., Rotenberg, E., Yakir, D., and Cohen, S.: The effect of spatial

628 resolution on the accuracy of leaf area index estimation for a forest planted in the desert transition
629 zone, Remote Sens. Environ., 109, 416-428, 2007.
630 Tian, Y., Dickinson, R. E., Zhou, L., Zeng, X., Dai, Y., Myneni, R. B., Knyazikhin, Y., Zhang, X., Friedl,
631 M., Yu, H., Wu, W., and Shaikh, M.: Comparison of seasonal and spatial variations of leaf area
632 index and fraction of absorbed photosynthetically active radiation from moderate resolution imaging
633 spectroradiometer (MODIS) and common land model, J. Geophys. Res, 109, D01103, 2004.
634 Tobin, B., Black, K., Osborne, B., Reidy, B., Bolger, T., and Nieuwenhuis, M.: Assessment of allometric
635 algorithms for estimating leaf biomass, leaf area index and litter fall in different- aged Sitka spruce
636 forests, Forestry, 79, 453-465, 2006.
637 Vitasse, Y., Delzon, S., Dufrêne, E., Pontailler, J. Y., Louvet, J. M., Kremer, A., and Michalet, R.: Leaf
638 phenology sensitivity to temperature in European trees: do within-species populations exhibit
639 similar responses, Agric. For. Meteorol., 149, 735-744, 2009.
640 Wood, S.: Generalized Additive Models: An introduction with R, Chapman & Hall, CRC, Boca Raton,
641 FL, USA, 8-15, 2006.
642 Woodgate, W., Jones, S. D., Suarez, L., Hill, M. J., Armston, J. D., Wilkes, P., Soto-Berelov, M.,
643 Haywood, A., and Mellor, A.: Understanding the variability in ground-based methods for retrieving
644 canopy openness, gap fraction, and leaf area index in diverse forest systems, Agric. For. Meteorol.,
645 205, 83-95, 2015.
646 Xiang, W., Fan, G., Lei, P., Zeng, Y., Tong, J., Fang, X., Deng, X., and Peng, C.: Fine root interactions

in subtropical mixed forests in China depend on tree species composition, Plant Soil, 395, 335-349, 2015.

Xiang, W. H., Hou, Y. N., Ouyang, S., Zhang, S. L., Lei, P. F., and Li, J. X.: Development of allometric equations for estimating tree component biomass of seven subtropical species in southern China, Eur. J. For. Res., in review, 2016.

Yao, D. D., Lei, X. D., Yu, L., Lu, J., Fu, L. Y., and Yu, R. G.: Spatial heterogeneity of leaf area index of mixed spruce-fir-deciduous stands in northeast China, Acta Ecol. Sinica, 1, 71-79, 2015. (in Chinese with English abstract)

655 **Table 1** Descriptive statistical characteristics of LAI values measured from April 2014 to January 2015

656 in *P. massoniana-L. glaber*, *C. axillaris* and *L. glaber-C. glauca* forests (*n*=100).

657

Measurement season	Forest type	Minimum value	Maximum value	Variance coefficient (%)	*P*-value of K-S test	Data transformation
	P. massoniana-L. glaber	1.29	4.03	27.5	0.021	0.275
January	*C. axillaris*	0.53	2.38	34.0	0.260	
	L. glaber-C. glauca	0.43	6.98	40.2	0.018	0.243
	P. massoniana-L. glaber	1.57	7.83	36.4	0.076	
April	*C. axillaris*	1.34	8.33	47.0	0.047	0.535
	L. glaber-C. glauca	1.34	10.22	59.6	0.000	0.158
	P. massoniana-L. glaber	1.56	8.16	38.0	0.003	0.075
July	*C. axillaris*	1.73	8.17	37.8	0.166	
	L. glaber-C. glauca	1.68	7.58	33.1	0.010	0.170
	P. massoniana-L. glaber	1.55	6.79	38.3	0.321	
October	*C. axillaris*	0.37	6.51	44.1	0.102	
	L. glaber-C. glauca	1.49	7.88	49.3	0.000	0.212

658

659

660

Table 2 Average woody to total leaf ration (α) and clumping index (Ω_E) values in *P. massoniana-L. glaber*, *C. axillaris* and *L. glaber-C. glauca* forests. Values in parenthesis are the standard deviation of α and Ω_E values (n=100).

Measurement season	Forest type	Mean value		Standard deviation	
		α	Ω_E	α	Ω_E
January	*P. massoniana-L. glaber*	0.06	0.88	0.04	0.09
	C. axillaris	0.15	0.92	0.09	0.08
	L. glaber-C. glauca	0.07	0.87	0.09	0.09
April	*P. massoniana-L. glaber*	0.08	0.87	0.05	0.09
	C. axillaris	0.07	0.85	0.06	0.10
	L. glaber-C. glauca	0.15	0.86	0.07	0.09
July	*P. massoniana - L. glaber*	0.07	0.87	0.04	0.09
	C. axillaris	0.04	0.90	0.03	0.07
	L. glaber-C. glauca	0.05	0.87	0.03	0.08
October	*P. massoniana-L. glaber*	0.09	0.85	0.10	0.08
	C. axillaris	0.14	0.87	0.14	0.10
	L. glaber-C. glauca	0.09	0.84	0.08	0.09

671 **Table 3** Semivariogram theoretical models and fitted parameters for LAI values in *P. massoniana-L. glaber* (90 m × 190 m irregular shape), *C. axillaris* (100 m × 100 m) and *L. glaber-C. glauca* (100 m × 100 m) forests.

674

Measurement season	Forest type	Model	Nugget (C_0)	Sill (C_0+C)	C/(C_0+C)	Range (A_0/m)	r^2	Residual sum of squares (RSS)
January	*P. massoniana-L. glaber*	Exponential	0.0068	0.0614	0.889	27.00	0.607	9.762×10^{-5}
	C. axillaris	Exponential	0.0030	0.1820	0.984	13.80	0.504	1.219×10^{-4}
	L. glaber-C. glauca	Gaussian	0.0029	0.1178	0.975	15.42	0.888	3.468×10^{-5}
April	*P. massoniana-L. glaber*	Exponential	0.1220	0.7670	0.841	17.70	0.229	0.017
	C. axillaris	Linear	0.1760	0.1760	0.000	52.96	0.189	1.762×10^{-4}
	L. glaber-C. glauca	Exponential	0.0008	0.0152	0.951	26.40	0.978	2.290×10^{-7}
July	*P. massoniana-L. glaber*	Linear	0.0843	0.0843	0.000	92.69	0.074	1.383×10^{-4}
	C. axillaris	Exponential	0.1460	0.9340	0.844	17.70	0.258	0.017
	L. glaber-C. glauca	Exponential	0.0065	0.0684	0.905	22.80	0.951	5.781×10^{-6}
October	*P. massoniana-L. glaber*	Exponential	0.1620	1.6310	0.901	11.70	0.173	0.017
	C. axillaris	Spherical	0.0050	0.5830	0.991	11.90	0.000	1.870×10^{-3}
	L. glaber-C. glauca	Exponential	0.0005	0.0125	0.960	21.90	0.894	4.444×10^{-7}

675

676

677

678 **Table 4** Estimated coefficients of the generalised additive models (GAMs) for the factors with effects

679 on LAI values measured in *P. massoniana-L. glaber*, *C. axillaris* and *L. glaber-C. glauca* forests.

680

Measurement season	Parameter	*F*-value	*P*-value	r^2	AIC
January	s (Stem number, 2)	16.716	<0.0001***	0.3481	655.91
	s (Crown coverage, 2)	4.545	0.034*		
	s (PESB, 2)	26.105	<0.0001***		
	s (PDSB, 2)	27.281	<0.0001***		
	factor(Forest types)	39.847	<0.0001***		
July	s (Stem number, 2)	5.027	0.026*	0.040	880.93
	s (PDSB, 2)	7.115	0.008**		

681

682 The significance of the regressions (*P*) are *, **, *** for *P*<0.05, 0.01, and 0.001, respectively

Figure captions

Fig. 1 Seasonal variation in mean LAI value (with standard deviation) in *P. massoniana-L. glaber*, *C. axillaris* and *L. glaber-C. glauca* forests. The different letters by values indicate significant differences (P<0.05) among measurement seasons in a given forest.

Fig. 2 Spatial heterogeneity map of LAI values interpolated through ordinary Kriging method for *P. massoniana-L. glaber*, *C. axillaris* and *L. glaber-C. glauca* forests.

Fig. 3 Partial effects of stem number, crown coverage (m^2), the proportion of evergreen conifer species to total stand BA (PESB), the proportion of deciduous species to total stand BA (PDSB) and forest types (calculated for overstorey trees with height larger than average stand height) on the LAI values observed in January in *P. massoniana-L. glaber*, *C. axillaris* and *L. glaber-C. glauca* forests.

Fig. 4 Partial effects of stem number and the proportion of deciduous species to total stand BA (PDSB) (calculated for overstorey trees with height larger than average stand height) on the LAI values observed in July in *P. massoniana-L. glaber*, *C. axillaris* and *L. glaber-C. glauca* forests.

Figure 1

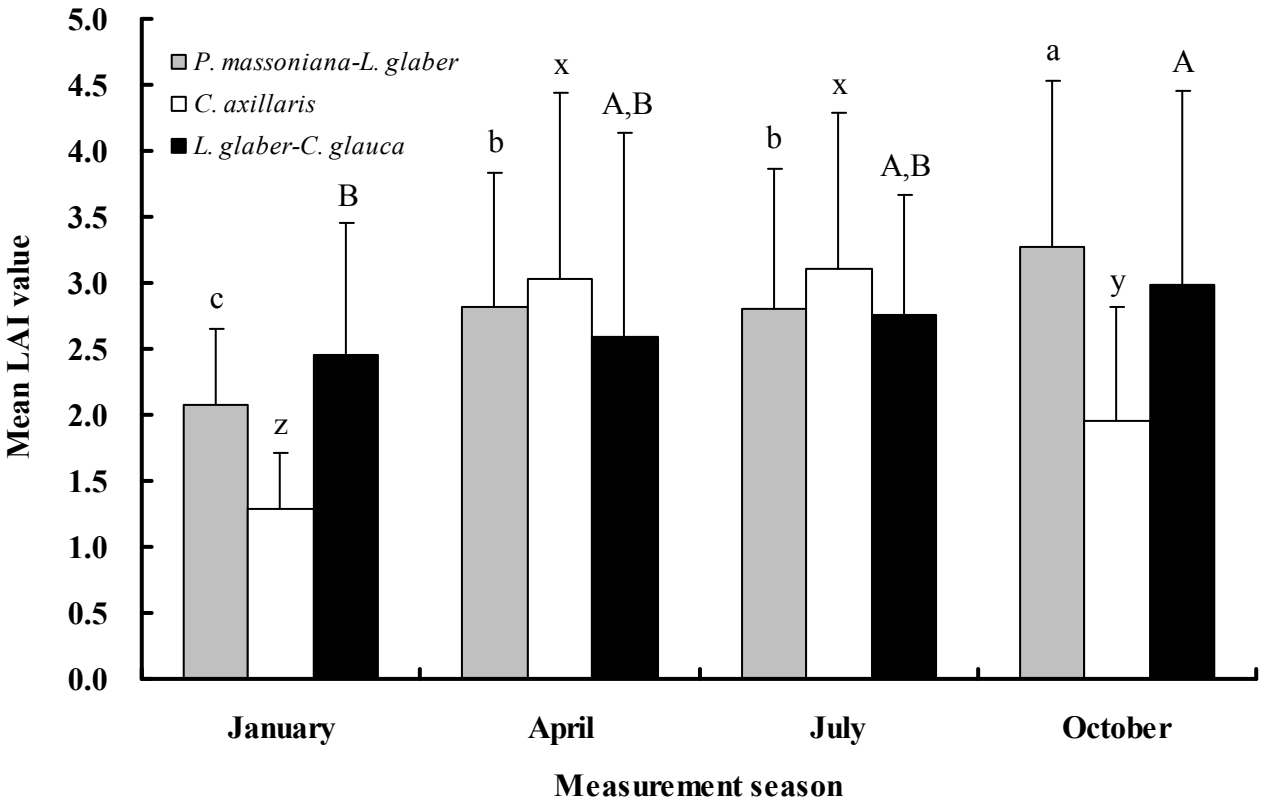
5.0
4.5
4.0
3.5
3.0
2.5
2.0
1.5
1.0
0.5
0.0
Mean LAI value
P. massoniana-L. glaber
C. axillaris
L. glaber-C. glauca
c
z
B
b
x
A,B
b
x
A,B
a
y
A
January
April
July
October
Measurement season

712 **Figure 2**

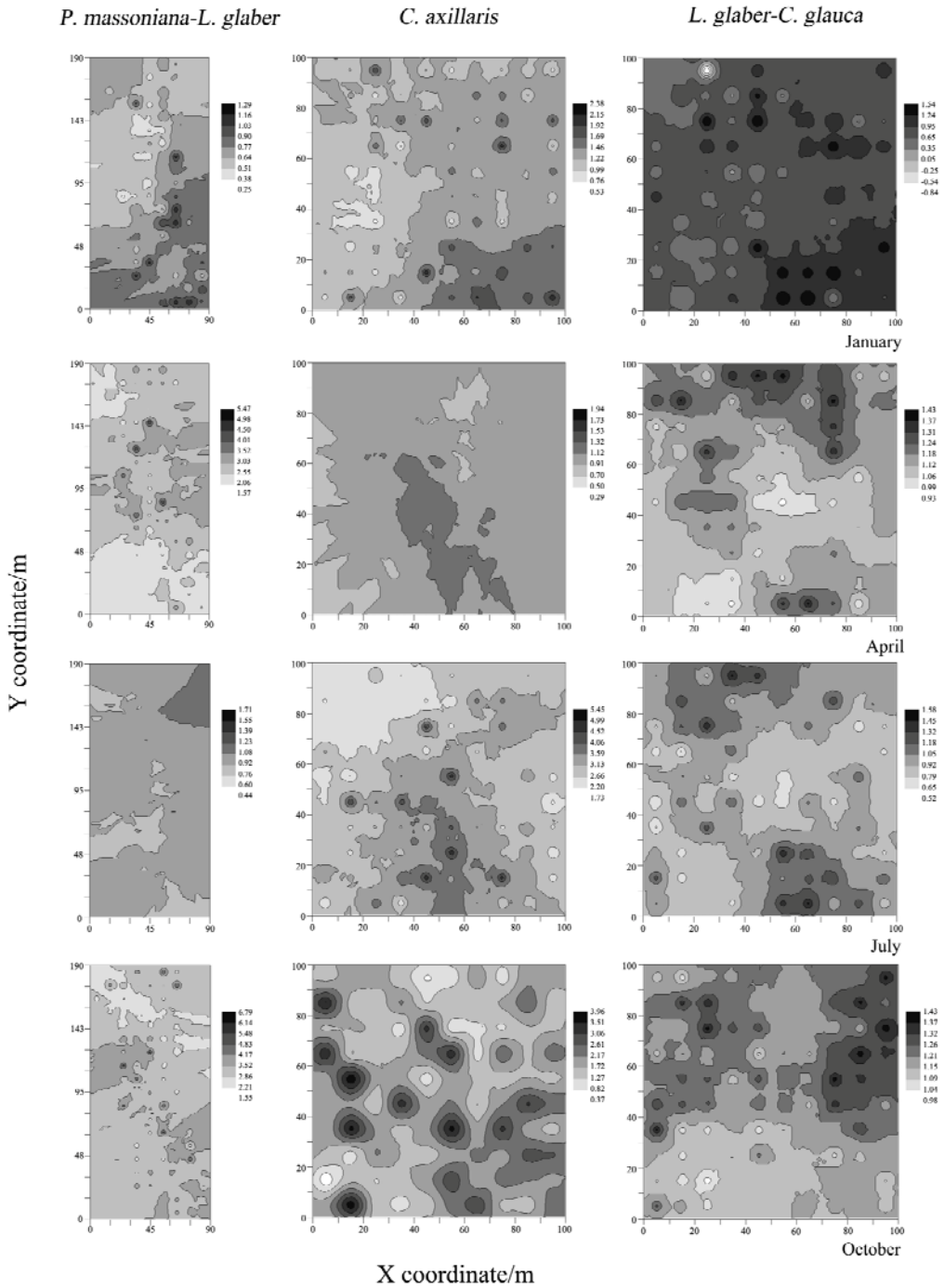

713

714

715 **Figure 3**

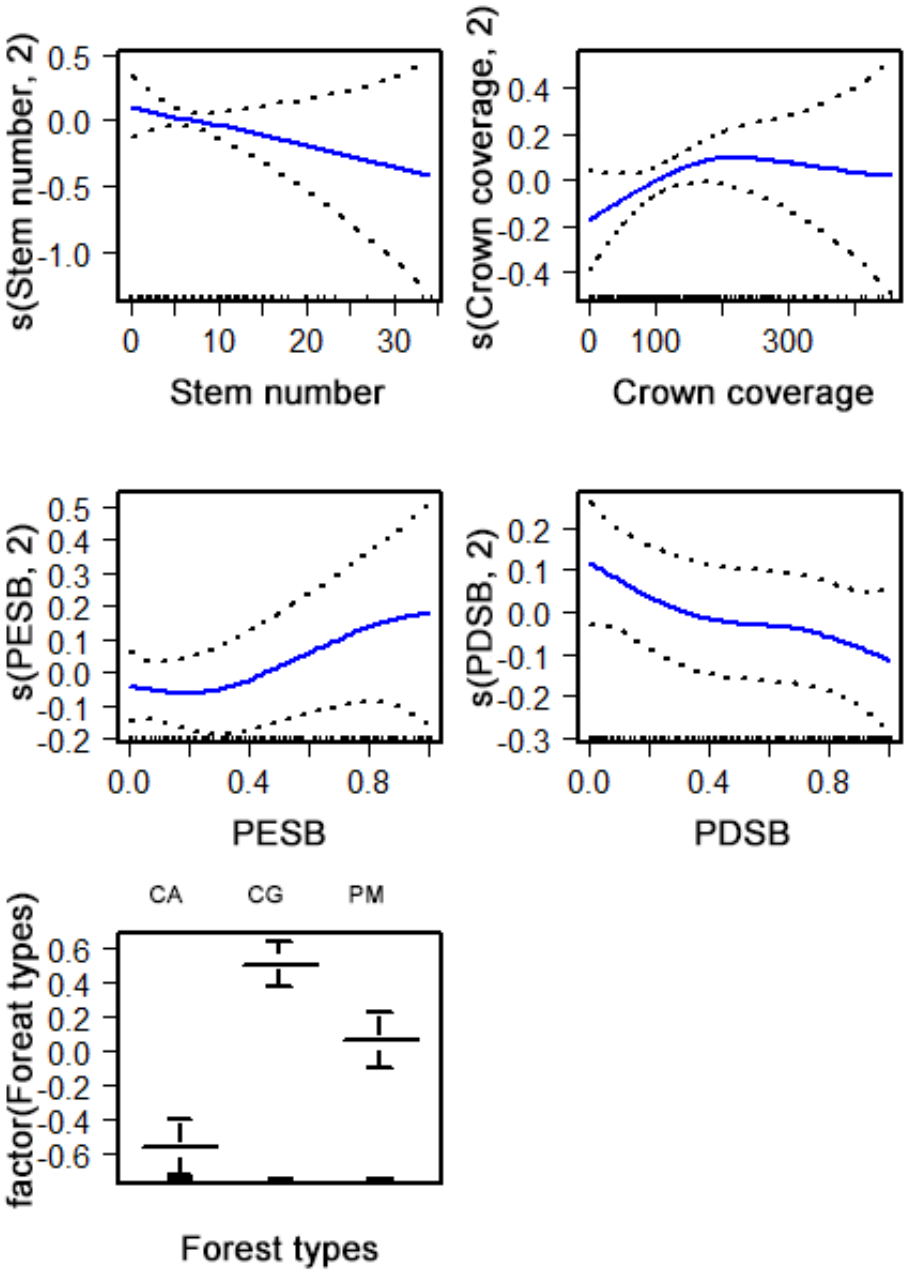

716

717

718

719 **Figure 4**

720

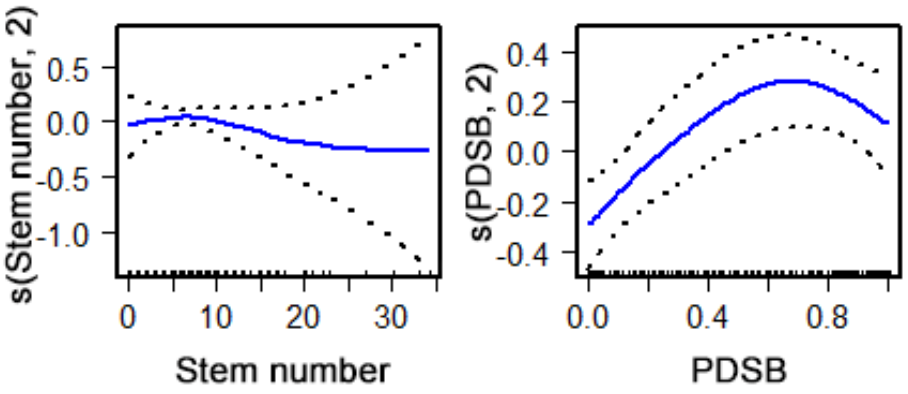

721